Chapter 2
"Prototypical" Optical Absorption Spectra of Phthalocyanines and Their Theoretical Background

In this chapter, the theoretical background of optical absorption spectra of phthalocyanines is described on the basis of their molecular orbitals (MOs). Note that because we attempted to describe the theoretical background without extreme mathematicization but as graphically as possible, some accuracy may have been sacrificed for comprehensibility. It is not our main purpose in this chapter to chronologically trace the progress of theoretical studies on phthalocyanines (and porphyrins); hence, some important milestone studies have been omitted. Readers interested in quantitative derivation should refer to the original papers. In this monograph, attention will be mostly focused on spectral properties in the solution phase. Exciton coupling between chromophores, which will be described in Sect. 3.2.4, is enhanced in the solid state; hence, the spectra are significantly broadened and become less structured. In the vapor phase, the molecules may be far apart; however, most of the phthalocyanines are involatile at room temperature and atmospheric pressure. Hence, as spectral measurements need to be carried out at considerably higher temperatures, the observed spectra may be rather broad as vibrational modes are highly activated. In solutions (regardless of their being organic or inorganic), phthalocyanines have quite a large molecular extinction coefficient at their most intense absorption band (on the order of 10^5 $M^{-1}cm^{-1}$), spectra of adequate quality are obtained from very dilute solutions (10^{-6} M), where the dye molecules are far apart (however, this depends on the compound and some compounds can form dimers or higher aggregates even in this concentration range as will be discussed in Sect. 3.2.4). It is true that interactions with solvent molecules need to be taken into consideration; however, the solvent effect is generally negligible unless the solvent used induces or takes part in certain chemical reactions with the phthalocyanines of interest (Sect. 3.2.7).

H. Isago, *Optical Spectra of Phthalocyanines and Related Compounds*,
NIMS Monographs, DOI 10.1007/978-4-431-55102-7_2

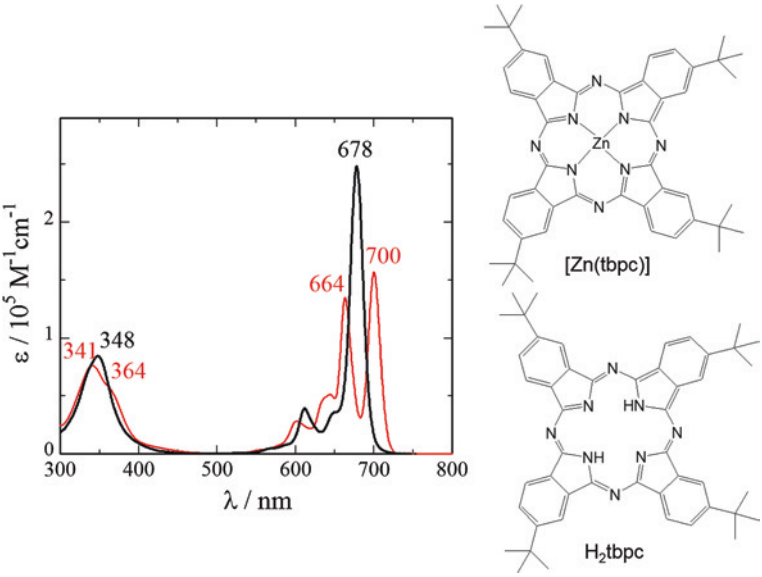

Fig. 2.1 Optical absorption spectra of [Zn(tbpc)] (*black solid line*) and H_2tbpc (*red broken line*) in chloroform. Only one regioisomer is shown for each compound

2.1 Prototypical Absorption Spectra of Phthalocyanines in Solutions

2.1.1 Prototypical Spectra of Phthalocyanines

Figure 2.1 shows the optical absorption spectra of zinc- and metal-free phthalocyanines in chloroform, represented as [Zn(tbpc)][1] and H_2tbpc, respectively. The macrocycles are substituted by four *tert*-butyl (^{t}Bu) groups to make them highly soluble in common organic solvents (particularly nonaromatic solvents, which are transparent in a wide spectral range). This substituent is very useful because it markedly improves the solubility of phthalocyanines in common organic solvents with negligible changes in their electronic structures and hence has been quite frequently used for spectroscopic investigation of phthalocyanines.[2]

The spectrum of [Zn(tbpc)] is typical of metallated phthalocyanines. It is characterized by (1) the appearance of an intense (log ε = ca. 5) absorption band at

[1]The "tbpc" is the abbreviation of tetra(*tert*-butyl)phthalocyaninate dianion (Sect. 1.2.2).

[2]Careful readers may be concerned that the tetrasubstituted phthalocyanines are mixtures of four regioisomers, as determined from the positions of the substituents. This is true. However, it is not important in most cases. One research group has successfully separated four regioisomers of tetrasubstituted phthalocyanines using an HPLC technique; however, they have determined that the difference in their spectral properties is negligible [1].

approximately 670 nm [generally termed the Q band (Sect. 2.1.2)] associated with some less intense (log ε = ca. 4) satellites at its blue flank (600–650 nm), (2) the appearance of a less intense but broad band at approximately 350 nm (generally called the Soret or B band), and (3) transparency in the other spectral regions (spectral windows). The spectral feature of H_2tbpc, apart from the splitting of the Soret and Q bands into two bands having nearly the same intensity instead of a single band observed for [Zn(tbpc)],[3] is essentially similar to that of [Zn(tbpc)]. Thus, both species absorb red light intensely and are transparent in the other spectral regions (400–600 nm and >750 nm). This is the reason why phthalocyanines show an intense blue color, as discussed in Sect. 1.1.2.

The spectral band widths for the two species are quite narrow ((484 cm^{-1} for [Zn(tbpc)], 357 (for the 700 nm band) and 408 cm^{-1} (for the 664 nm band) for H_2tbpc) as compared with that for methylene blue (1233 cm^{-1}; Fig. 1.3). This suggests that their molecular structures are more rigid than that of methylene blue and their structures in the lowest excited state do not markedly differ from those in the ground state (Sect. 1.1.5).

Before considering the origin of the absorption bands, let us compare the spectra of phthalocyanines with those of the other dyes that have a similar cyclic tetrapyrrole skeleton.

2.1.2 Comparison with Spectra of Similar Tetrapyrrole Macrocycles

Figure 2.2 (left) shows the optical absorption spectra of metal complexes of the phthalocyanine derivative (Pc[4]; [Cu(tbpc)]), tetraazaporphyrin derivative (TAP), tetraphenylporphyrin (TPP), and tetrabenzoporphyrin derivative (TBP) as well as metal-free chlorin e6 (their structures are shown in Fig. 2.2 (right)). All the spectra are plotted with their most intense band normalized. The spectra of TPP and Pc are markedly different in spite of the similarity in their tetrapyrrole skeletons. The TPP spectrum shows an intense band at approximately 400 nm and very weak bands at approximately 550 nm, which are generally termed the Soret and Q bands, respectively. On the other hand, the spectrum of Pc, which is typical of metal complexes of phthalocyanines (Sect. 2.1.1), shows the most intense band at approximately 670 nm and much less intense band at approximately 350 nm. This difference cannot be attributed to the expansion of the π-conjugation system at the four fused benzo groups in Pc. Ring expansion from TPP to TBP (Fig. 2.2 (right)) gives rise to a slight shift at the Soret-band position.[5] Comparison between these four similar macrocycles has shown that TAP and TBP can be considered to be structural intermediates

[3]The split Soret and Q bands of H_2tbpc are attributed to the symmetry-lowering effect based on the presence of imino protons in the cavity, as described in Sect. 2.2.9.

[4]In this subsection, as the central elements do not play a crucial role, they are not specified in the abbreviations of the macrocyclic compounds.

[5]The peripheral substituents are omitted for clarity in this discussion.

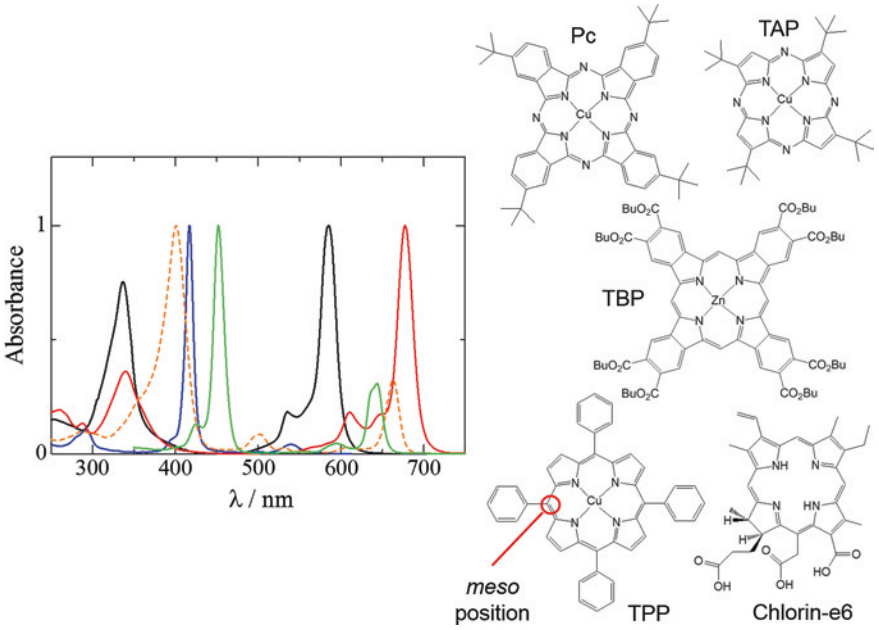

Fig. 2.2 Optical absorption spectra of Pc in dichloromethane (*red solid line*), TPP in dichloromethane (*blue solid line*), TAP in dichloromethane (*black solid line*), TBP in DMF (*green solid line*) [2], and chlorin e6 in ethanol (*orange broken line*) [3].The spectra of TBP (*right*) and chlorin e6 (*left*) were redrawn from digital data available at the web site of "PhotochemCAD" (http://omlc.ogi.edu/spectra/PhotochemCAD/index.html) with permission. *Source for the other species* NIMS eSciDoc—IMEJI. © Hiroaki Isago with CC-BY-NC 3.0 license

between TPP and Pc. Substitution of the phenyl-substituted methyne (C-phenyl) groups at "*meso*-positions" (see TPP for the *meso*-position) in TPP with nitrogen atoms generates TAP, fusion of benzo groups to the periphery of the four pyrrole rings generates TBP, and both generate Pc. Interestingly, the spectral characteristics of TAP and TBP are also intermediate of those of the other two. In the case of TBP, upon fusion of a benzo group to the periphery of each of the pyrrole ring, the Soret band is slightly shifted, as mentioned above; however, a new band appears at approximately 630 nm, which resembles the Q band in the Pc spectrum. On the other hand, the modification of TPP to TAP brings about a significantly increased Q band intensity and caused a large blue-shift in the Soret-band position. Thus, it seems that the introduction of nitrogen atoms into the innermost 16-membered ring has greater effects on the electronic structure of the macrocycle than the fusion of benzene rings to the periphery of the pyrrole rings. It is noteworthy that chlorin e6 shows a spectrum similar (Fig. 2.2 (left)) to that of the TPP derivative notwithstanding the disruption of the π conjugation system at the peripheral ethylene bridge.[6]

[6]In contrast, disruption of the π-conjugation system in the innermost 16-membered ring of phthalocyaninate leads to the disappearance of the characteristic Q band (one or more broad bands are observed in the 400–500 nm region, instead) [4].

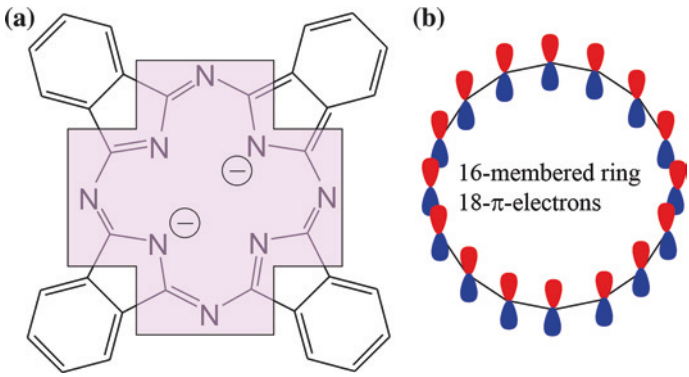

Fig. 2.3 **a** Innermost 16-membered ring in a phthalocyanine molecule and **b** dianion of ideal cyclic polyene, $C_{16}H_{16}^{2-}$ as starting model. *Source* NIMS eSciDoc-IMEJI. © Hiroaki Isago with CC-BY-NC 3.0 license

Therefore, to understand the optical absorption spectra and electronic structure of phthalocyanines, we may assume that (1) the same method applied to porphyrins can also be applied to phthalocyanines, (2) the innermost 16-membered ring should be the starting point (Fig. 2.3a), and (3) introduction of nitrogen atoms into the 16-membered ring and fusion of benzene rings play crucial roles in determining the balance in intensity between the Soret and Q bands.

In the following subsection, some representative MO models will be discussed to better understand the electronic structures of porphyrins, phthalocyanines, and other related macrocycles that exhibit the absorption spectra as shown in Fig. 2.2.

2.2 Molecular Orbital Models of Porphyrins and Phthalocyanines

2.2.1 Selection Rule in Optical Absorption (Optical Absorption = Generation of Vector)

Before considering MO models, it may be feasible to consider a selection rule dictating that the transition from the ground state to a given excited state involves optical absorption. In Chap. 1, it has been briefly mentioned that when a dye molecule is excited via optical absorption, the distribution of electrons changes in the molecule, which generates an electric dipole. That is, the molecule cannot be excited via optical absorption to higher states unless the transition involves generation of an electric dipole moment. Thus, absorption of light is equal to generation of a vector. Keeping this in mind, apparently complex phenomena, such as configuration interaction (Sect. 2.2.6) and exciton coupling (Sect. 3.2.4.2), may be understood more easily.

2.2.2 Perimeter Model

To understand optical absorption spectra and the electronic structures of porphyrins and related macrocyclic compounds, Simpson has proposed a simple "free-electron" model, in which 18 π-electrons are circulating along the periphery of the innermost 16-membered ring [5]. Note that two excess electrons of the macrocyclic ligand (in metal complexes, porphyrins and phthalocyanines may be regarded as dianions) in addition to the 16 π-electrons from each atom of the innermost 16-membered ring (Fig. 2.3a) are included in this model. Therefore, the dianion of an ideal 16-membered alternant cyclic polyene, $C_{16}H_{16}^{2-}$, has aromaticity according to Hückel's "4n + 2" rule. We use this as the starting model (Fig. 2.3b).

Let us consider the motion of a free electron circulating along the periphery of a 16-membered ring as a function of angle, ϕ (Fig. 2.4a). The k value is taken as positive when the electron is circulating clockwise and negative when it is circulating counterclockwise. The wave function Ψ_k for the electron with an angular momentum of k is represented by the following differential equations (Eqs. 2.1 and 2.2), where m, E_k, and $\hbar$ denote the mass and energy of the electron, and the Planck constant, respectively.

$$\frac{\partial^2 \Psi_k}{\partial \phi^2} = -\frac{2mE_k}{\hbar^2}\Psi_k; \quad E_k = k^2(\hbar^2/2m) \tag{2.1}$$

$$\frac{\hbar}{i}\frac{\partial \Psi_{\pm k}}{\partial \phi} = \pm k\hbar\Psi_{\pm k} \tag{2.2}$$

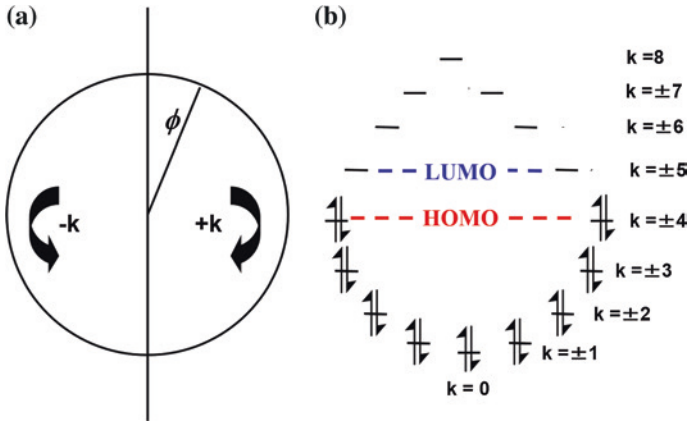

Fig. 2.4 **a** Perimeter model: a free electron circulating along the periphery of the 16-membered ring with an angular momentum of k (clockwise) and $-k$ (counterclockwise) and **b** energy levels of wave functions (MOs) for electrons with various k values. *Source* NIMS eSciDoc—IMEJI. © Hiroaki Isago with CC-BY-NC 3.0 license

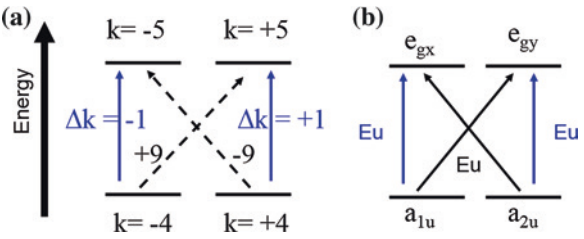

Fig. 2.5 Schematic diagrams of electronic transitions from HOMO to LUMO (straight transitions are shown as *blue arrows* and cross transitions as *black arrows*) in the perimeter model (**a**) and those of the "descent-in-symmetry" model (**b**). The *solid and broken arrows* denote allowed and forbidden transitions, respectively

The solution is given in a complex form as (Eq. 2.3).

$$\Psi_{\pm k} = \frac{1}{\sqrt{2}} \exp(\pm ik\phi); \quad (k = 0, 1, 2, \ldots 7, 8) \tag{2.3}$$

As each wave function has the same value for ϕ and $\phi + 2\pi$, (i.e., $\Psi(\phi) = \Psi(\phi + 2\pi)$), k must be an integer. As the energy of Ψ_k (E_k) is proportional to the square of k values and each orbital accepts up to two electrons, the orbitals with $k = 0$, ±1, ±2, ±3, and ±4 are occupied by electrons in the ground state. Thus, $\Psi_{\pm4}$ and $\Psi_{\pm5}$ are the HOMOs and LUMOs,[7] respectively (Fig. 2.4b). Note that the orbitals $\Psi_{\pm k}$ are degenerate because they are at the same energy level, only the direction of circulation is different. Therefore, there are four possible transitions from the HOMOs to the LUMOs. One set includes straight transitions (Ψ_{+4} to Ψ_{+5} and Ψ_{-4} to Ψ_{-5}) and another set includes cross transitions (Ψ_{+4} to Ψ_{-5} and Ψ_{-4} to Ψ_{+5}). The change in k during the transition is ±1 in the straight transitions whereas it is ±9 in the cross transitions (Fig. 2.5a). Of these two sets of transitions, only the former one is allowed because these transitions involve the generation of an electric dipole moment, as shown below.

Let us assume that the 16-membered ring is located parallel to the x,y-plane. Consequently, the wave functions consist of atomic p_z orbitals, which are perpendicular to the molecular plane. Cartesian coordinates (x, y) are presented using polar coordinates (r, ϕ) as ($r\cos\phi$, $r\sin\phi$). When the dipole moment is generated along the x-axis, the Cartesian coordinate x is presented as a function of ϕ (Eq. 2.4).

$$x = r\cos\phi = \frac{1}{2}\{\exp(i\phi) + \exp(-i\phi)\} \tag{2.4}$$

As optical absorption occurs only when an electric dipole is generated, the following integral must be non-zero through the transition from Ψ_k to Ψ_n (Eq. 2.5).

$$\int_0^{2\pi} \Psi_k r \Psi_n^* d\phi = \int_0^{2\pi} \{\exp(+ik\phi) x \exp(-in\phi)\} d\phi \tag{2.5}$$

[7]Refer to Sect. 1.1.4 for the definitions of HOMO and LUMO.

As x is represented by Eqs. 2.4 and 2.5 includes the following two integral calculations (Eq. 2.6), either of which must be non-zero.

$$\int_0^{2\pi} [\exp\{(+k+1-n)i\phi\}]d\phi + \int_0^{2\pi} [\exp\{(+k-1-n)i\phi\}]d\phi \neq 0 \qquad (2.6)$$

Therefore, the change in k (Δk; i.e., $n - k$) through the transition must be ± 1. Similarly, the change in k caused by the generation of an electric dipole moment along the y-axis must also be ± 1. However, it is determined that another set of transition values ($\Delta k = \pm 9$) are forbidden. This successfully explains the appearance of a very intense Soret band ($\Delta k = \pm 1$) and a very weak Q band ($\Delta k = \pm 9$) in the spectra of porphyrins (Fig. 2.2). The large change in Δk (± 9) for the Q band has also been evidenced by a magnetic circular dichroism study (Sect. 2.2.8). However, the energy profile (i.e., which of the two sets of transitions requires a higher energy?) cannot be explained by this model.

2.2.3 Graphical Description of Molecular Orbitals

As the wave functions described above include imaginary parts, they are not suitable for graphical representation of the MOs. Linear combination of a set of Ψ_{+k} and Ψ_{-k} can represent them in a form of trigonometric functions (Eq. 2.7).

$$\frac{\Psi_{+k} + \Psi_{-k}}{\sqrt{2}} = \cos(k\phi); \quad \frac{\Psi_{+k} - \Psi_{-k}}{\sqrt{2}i} = \sin(k\phi) \qquad (2.7)$$

Figure 2.6 shows some examples of wave functions with only their phase taken into consideration. When $k = 0$, all the atomic p_z orbitals have the same phase (i.e., the same color[8]); hence, the wave function Ψ_0 has no nodal plane.[9] When $k = \pm 1$, the phase (sign) of the wave function is inversed at the 0th and 8th atoms for the sine form and at the 4th and 12th atoms for the cosine counterpart; hence, there is one nodal plane. Similarly, wave functions with $k = \pm 2$ have two nodal planes. Thus, the number of nodal planes increases with increasing absolute value of k. Readers may have determined that the two wave functions $\Psi_{\pm k}$ are identical upon appropriate rotation (for example, in the case of $k = \pm 1$, $\sin\phi$ is equivalent to $\cos\phi$ upon clockwise rotation by 90°). This is because they are degenerate. Note that the linear combination of $\Psi_{\pm 8}$ similarly produces sine and cosine forms, but only one wave function (the cosine form in this case) makes sense because all the 16 atoms are located on nodes in its counterpart. What is most important in this discussion is that

[8]Even though there seems to be no red or blue color between neighboring atoms, it may be assumed that a considerable amount of π-cloud is present when the atoms have the same sign (color).

[9]Note that a nodal plane is present on the molecular plane (because of the nature of the p_z orbital) but this is not taken into account here.

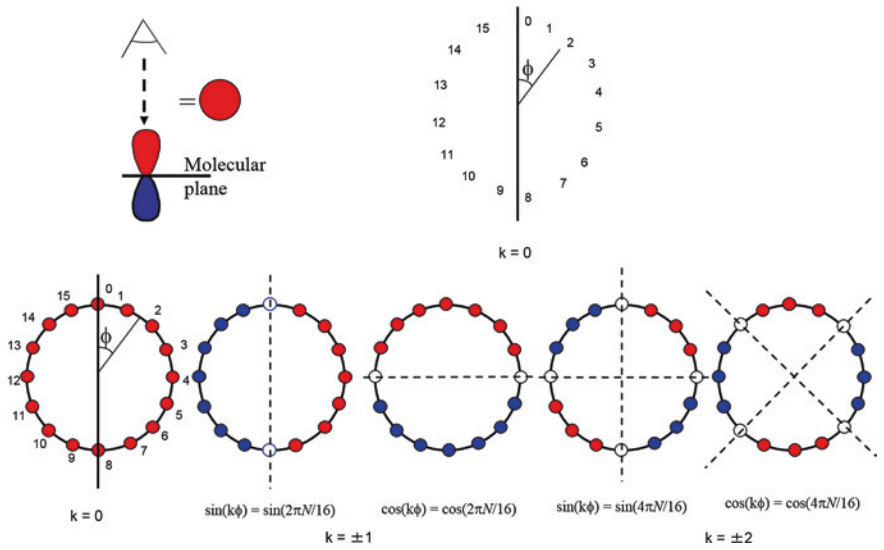

Fig. 2.6 Graphical illustrations of the lowest five π MOs (k = 0, ±1, ±2) based on perimeter model. The *red and blue closed circles* denote the phases of the MOs (the positive and negative signs are denoted by *red and blue circles*, respectively). Only the signs of the wave function are shown; hence, the size of the circles does not represent the amplitude of the coefficient). *Source* NIMS eSciDoc—IMEJI. © Hiroaki Isago with CC-BY-NC 3.0 license

both the HOMOs ($\Psi_{\pm 4}$) and LUMOs ($\Psi_{\pm 5}$) are degenerate in an ideal 16-membered cyclic polyene belonging to the D_{16h} point group (in group theory), as shown in Fig. 2.7 (top). In this symmetry, the HOMOs and LUMOs are both degenerate and belong to the following irreducible representations, e_{4u} and e_{5g}, respectively.

2.2.4 "Descent-in-Symmetry" Model

Neither porphyrins nor phthalocyanines actually belong to D_{16h} because of the presence of the nitrogen atoms and the four peripheral C_2H_2 bridges. These modifications decrease the symmetry of the parent 16-membered cyclic polyene, D_{16h}, to D_{4h}, which corresponds to the actual molecular symmetry point group of a common porphyrin [6]. Therefore, the perimeter model requires further modifications. Following the decrease in the symmetry, the degeneracy is lifted for the HOMOs (a_{1u} and a_{2u}; Fig. 2.7 bottom), whereas it is maintained for the LUMOs (e_g). The a_{1u} HOMO is characterized by the presence of nodes at all the *meso*-positions and pyrrole nitrogen atoms. However, the a_{2u} counterpart has a large amplitude at the same positions and has nodes between these positions. The a_{2u} orbital is stabilized owing to the presence of the high electron density at atoms of large electronegativity (nitrogen) whereas the a_{1u} orbital is stabilized by a strong bonding interaction between the innermost 16-membered alternant polyene and the peripheral ethylene

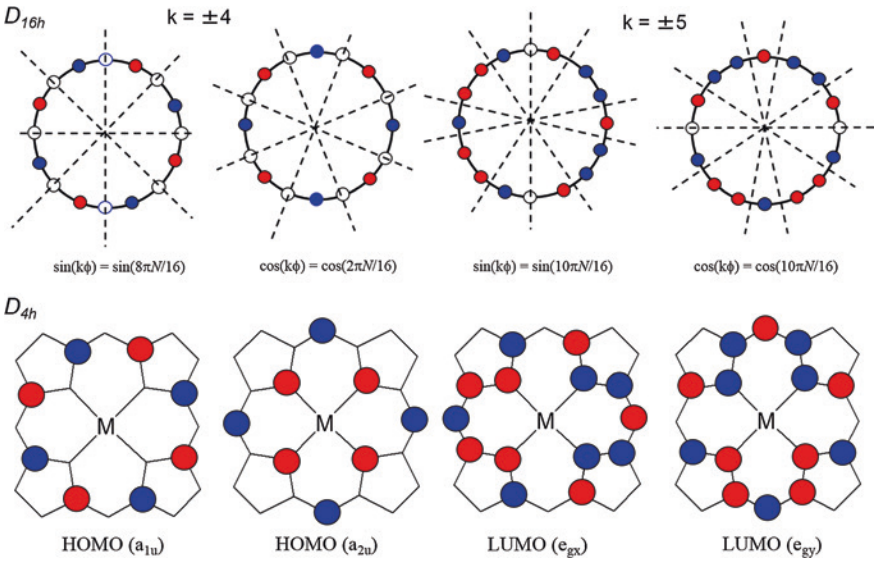

Fig. 2.7 Graphical illustrations of HOMO (k = ±4) and LUMO (k = ±5) based on perimeter model (*top*) and descent-in-symmetry model (*bottom*). The *red and blue closed circles* denote phases of the MOs (the positive and negative signs are denoted by *red and blue circles* respectively). Only the signs of the wave function are shown; hence, the size of the circles does not represent the amplitude of the coefficients). *Source* NIMS eSciDoc—IMEJI. © Hiroaki Isago with CC-BY-NC 3.0 license

moieties.[10] In the case of porphyrins, these two effects are even; hence, the two orbitals are still nearly degenerate (accidental degeneracy).

The four HOMO-LUMO transitions under the D_{4h} symmetry are shown in Fig. 2.5b. In this modified model, the $a_{2u} \rightarrow e_g$ transition has a symmetry of E_u ($A_{2u} \times E_g = E_u$[11]) and the $a_{1u} \rightarrow e_g$ transition also has the same symmetry ($A_{1u} \times E_g = E_u$; Sect. 2.2.5). The problem with this model is that both the transitions are allowed (x,y-polarized); hence, the weak Q band in the spectrum of porphyrin cannot be explained.

2.2.5 How to Use Character Tables (for Group Theory)

The purpose of this discussion is not to explain the group theory but how to determine when an electronic transition of interest is allowed or forbidden using only a character table. At the end of Sect. 2.2.4, it has been demonstrated that the $a_{1u} \rightarrow e_g$

[10]Note that all the ethylene moieties are isolated from the innermost 16-membered ring in a_{2u} by nodes.

[11]In general, irreducible representations starting with a capital letter stand for a "state", whereas those starting with a small letter represent MOs.

transition is allowed (*x*,*y*-polarized). It is easy to determine an allowed transition using this table and some basic mathematical operations. Therefore, readers who are already familiar with this method may skip this subsection.

Readers are reminded that optical absorption (i.e., allowed electronic transition) is equal to the generation of a vector. Let us consider whether an electron transition from the Ψ_k orbital to Ψ_n is allowed or forbidden. For this transition to be allowed, the integral expression (Eq. 2.8, where *r* denotes the electric dipole moment) must be non-zero. Therefore, the triple product of Ψ_k, *r* (which is a radius vector), and Ψ_n must include a totally symmetric irreducible representation (which has all characters = +1; e.g., A_{1g} in D_{4h}: see Table 2.1). Assume that Ψ_k and Ψ_n belong to the irreducible representations a_{2u} and e_g, respectively. As the direct product of A_{2u} and E_g makes E_u (see the bottom row of Table 2.1), the irreducible representation of *r* must also be E_u to generate the A_{1g} representation as the result of the triple product (Table 2.2). As the E_u representation transforms (x, y) as shown in the rightmost column of the character table, this transition is allowed and *x*/*y*-polarized. However, a transition from a_{2u} to b_{1g} is determined to be forbidden because their direct product makes B_{2u} (Table 2.2), which cannot transform to any of *x*, *y*, *z*. Similarly, the $e_u \rightarrow e_u$ transition is also forbidden.

$$\int_{-\infty}^{\infty} \Psi_k r \Psi_n^* dv \neq 0 \tag{2.8}$$

Tables 2.1 and 2.3 show the character tables for the point groups D_{4h} and D_{2h}, to which the actual metallated and metal-free Pcs belong, respectively. Attention should be paid to the rightmost column, where basis functions of each irreducible representation are given. It has been determined that, of the ten irreducible representations (given in the leftmost column) in D_{4h}, only A_{2u} and E_u have a linear basis function ((x, y) and z, respectively). Similarly in D_{2h}, only B_{1u} (z), B_{2u} (y), and B_{3u} (x) have a linear basis function. Thus, *r* must belong to the irreducible

Table 2.1 Character table for D_{4h} point group

	E	$2C_4$	C_2	$2C'_2$	$2C''_2$	i	$2S_4$	σ_h	$2\sigma_v$	$2\sigma_d$	
A_{1g}	1	1	1	1	1	1	1	1	1	1	$x^2 + y^2, z^2$
A_{2g}	1	1	1	−1	−1	1	1	1	−1	−1	Rz
B_{1g}	1	−1	1	1	−1	1	−1	1	1	−1	$x^2 - y^2$
B_{2g}	1	−1	1	−1	1	1	−1	1	−1	1	xy
E_g	2	0	−2	0	0	2	0	−2	0	0	(Rx, Ry), (xz, yz)
A_{1u}	1	1	1	1	1	−1	−1	−1	−1	−1	
A_{2u}	1	1	1	−1	−1	−1	−1	−1	1	1	z
B_{1u}	1	−1	1	1	−1	−1	1	−1	−1	1	
B_{2u}	1	−1	1	−1	1	−1	1	−1	1	−1	
E_u	2	0	−2	0	0	−2	0	2	0	0	(x, y)
A_{2u} x E_g	1 × 2 = 2	1 × 0 = 0	1 × (−2) = −2	−1 × 0 = 0	−1 × 0 = 0	−1 × 2 = −2	−1 × 0 = 0	−1 × (−2) = 2	1 × 0 = 0	1 × 0 = 0	

Table 2.2 Product table for D_{4h} point group

	A_{1g}	A_{2g}	B_{1g}	B_{2g}	E_g	A_{1u}	A_{2u}	B_{1u}	B_{2u}	E_u
A_{1g}	A_{1g}	A_{2g}	B_{1g}	B_{2g}	E_g	A_{1u}	A_{2u}	B_{1u}	B_{2u}	E_u
A_{2g}	A_{2g}	A_{1g}	B_{2g}	B_{1g}	E_g	A_{2u}	A_{1u}	B_{2u}	B_{1u}	E_u
B_{1g}	B_{1g}	B_{2g}	A_{1g}	A_{2g}	E_g	B_{1u}	B_{2u}	A_{1u}	A_{2u}	E_u
B_{2g}	B_{2g}	B_{1g}	A_{2g}	A_{1g}	E_g	B_{2u}	B_{1u}	A_{2u}	A_{1u}	E_u
E_g	E_g	E_g	E_g	E_g	$A_{1g}+A_{2g}+B_{1g}+B_{2g}$	E_u	E_u	E_u	E_u	$A_{1u}+A_{2u}+B_{1u}+B_{2u}$
A_{1u}	A_{1u}	A_{2u}	B_{1u}	B_{2u}	E_u	A_{1g}	A_{2g}	B_{1g}	B_{2g}	E_g
A_{2u}	A_{2u}	A_{1u}	B_{2u}	B_{1u}	E_u	A_{2g}	A_{1g}	B_{2g}	B_{1g}	E_g
B_{1u}	B_{1u}	B_{2u}	A_{1u}	A_{2u}	E_u	B_{1g}	B_{2g}	A_{1g}	A_{2g}	E_g
B_{2u}	B_{2u}	B_{1u}	A_{2u}	A_{1u}	E_u	B_{2g}	B_{1g}	A_{2g}	A_{1g}	E_g
E_u	E_u	E_u	E_u	E_u	$A_{1u}+A_{2u}+B_{1u}+B_{2u}$	E_g	E_g	E_g	E_g	$A_{1g}+A_{2g}+B_{1g}+B_{2g}$

Table 2.3 Character table for D_{2h} point group

	E	C_2 (z)	C_2 (y)	C_2 (x)	I	σ(xy)	σ(xz)	σ(yz)	Linear, rotations quadratic
A_g	1	1	1	1	1	1	1	1	x^2, y^2, z^2
B_{1g}	1	1	−1	−1	1	1	−1	−1	Rz, xy
B_{2g}	1	−1	1	−1	1	−1	1	−1	Ry, xz
B_{3g}	1	−1	−1	1	1	−1	−1	1	Rx, yz
A_u	1	1	1	1	−1	−1	−1	−1	
B_{1u}	1	1	−1	−1	−1	−1	1	1	z
B_{2u}	1	−1	1	−1	−1	1	−1	1	y
B_{3u}	1	−1	−1	1	−1	1	1	−1	x

representation(s) that transform as (the translations) x, y, z, as shown in the character tables when the transition involves optical absorption.

2.2.6 *Gouterman's "Four-Orbital" Model*

Gouterman and coworkers have introduced the concept of "configuration interaction" between the two types of transition involving the doubly degenerate LUMO and two nearly degenerate HOMOs (hence, the four-orbital model) to explain the spectra of porphyrins [7–9]. Before considering this model, it should be again remembered that optical absorption is equal to the generation of a vector (an electric dipole moment). The "*x*, *y*-polarized degenerate excited state" means that the *x*-polarized (the generated dipole is parallel to the *x*-axis) and *y*-polarized excited states are at exactly the same energy level. As stated in Sect. 2.2.4, both the $a_{1u} \rightarrow e_g$ and $a_{2u} \rightarrow e_g$ transitions belong to the same symmetry, E_u. The "same irreducible representation" means that these electric dipole moments generated through the transitions have the same direction. Therefore, the conventional

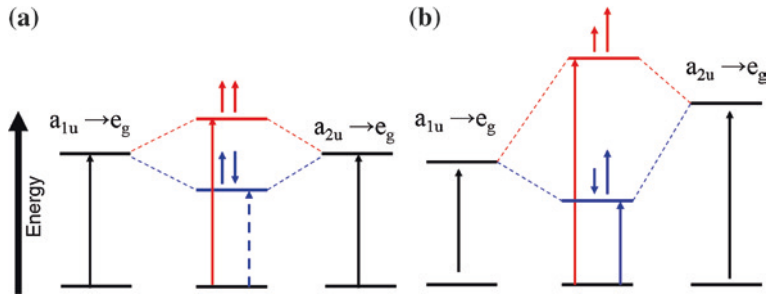

Fig. 2.8 Schematic diagrams of the four-orbital model for (**a**) porphyrins in which a_{1u} and a_{2u} orbitals are nearly degenerate and (**b**) phthalocyanines in which a_{2u} orbital is stabilized relative to a_{1u} counterpart. The energy scales are arbitrary

additivity rule for vectors may be applied to the dipole moments (i.e., they are enhanced when they are parallel and cancelled when they are antiparallel). In particular, the *x*-polarized $a_{2u} \rightarrow e_g$ and the *x*-polarized $a_{1u} \rightarrow e_g$ transitions have essentially the same energy (similar to the *y*-polarized transitions), because the a_{1u} and a_{2u} orbitals are nearly degenerate, and the two vectors strongly interact with each other.

Figure 2.8 shows schematic illustrations of the configuration interaction between the two types of transition. When the two dipole moments are parallel, the resultant energy level is higher than that of a single transition because of electric repulsion between the dipoles. The intensity increases because the two vectors are constructive. However, when they are antiparallel, the excited state is stabilized owing to electric attraction, but the spectral intensity is significantly reduced because the dipole moments have disappeared (cancelled by each other). This model predicts the appearance of an intense (Soret) band at a high energy and a very weak (Q) band at a low energy, as observed in the actual spectra of porphyrins (Fig. 2.2; blue solid line).[12]

2.2.7 Why Are the Spectra of Phthalocyanines Different from Those of Porphyrins in Spite of Their Similar Structures?

Figure 2.3 shows the absorption spectra of porphyrin (TPP) and the related macrocycles. The ring expansion (TBP) and substitution of *meso*-carbon atoms with nitrogen atoms (TAP) results in a significant increase in the intensity of the Q

[12]This description is rather qualitative and oversimplified. The MO wave function shown in Figs. 2.7 and 2.8 are converted by linear combinations of their complex forms (Eq. 2.7). Readers who are interested in strict, quantitative derivation should refer to the original papers [6–9].

band. This demonstrates that these modifications upset the balance of energy level between the occupied frontier orbitals (a_{1u} and a_{2u}). For example, substitution of *meso*-carbon with nitrogen significantly stabilizes the a_{2u} orbital relative to the a_{1u} counterpart (Sect. 2.2.4). Consequently, as their transition energy is no longer the same ($a_{1u} \rightarrow e_g < a_{2u} \rightarrow e_g$), the electric dipole moment of the lower excited state is not completely cancelled. Fusion of the benzo groups to the periphery of TAP also enhances the energy imbalance so that the Q band is intensified.

2.2.8 *Degeneracy of Excited States and Magnetic Circular Dichroism (MCD) Spectroscopy*

In the free-electron model, the degenerate orbitals have been demonstrated as pairs of orbitals with the same angular momentum but with different circulation directions (that is, clockwise ($+k$) and counterclockwise ($-k$) circulation). The two orbitals have the same energy, which depends on k^2 alone, in the absence of a magnetic field. The circulation of the electron is equal to the ring current of the opposite direction (that is, clockwise circulation = counterclockwise ring current), generating an upside magnetic moment (Fig. 2.9). Likewise, the counterclockwise circulation generates a downside magnetic moment of the same magnitude. Once an external magnetic field is applied perpendicularly to the molecular plane, the two orbitals are no longer equivalent in energy level and the degeneracy is lifted owing to the Zeeman effect to a much smaller extent than to the symmetry-lowering effects.

MCD spectroscopy is a powerful tool for investigating the electronic structure of molecules with high symmetry, such as porphyrins or phthalocyanines, because it provides valuable information on their degenerate states. MCD spectra can be measured using a conventional circular dichroism (CD) spectrometer that can be

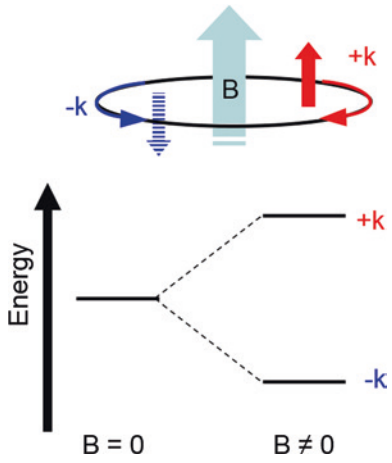

Fig. 2.9 Schematic illustration of degeneracy of MOs (in free-electron model) in the absence of external magnetic field and its disruption upon application of external magnetic field. *Source* NIMS eSciDoc—IMEJI. © Hiroaki Isago with CC-BY-NC 3.0 license

equipped with an electromagnet or even a permanent magnet in its sample compartment. The magnetic field is oriented parallel to the optical propagation (that is, in the Faraday arrangement). In this orientation, only transitions between states with different angular magnetic quantum numbers (ΔJ) of unity can absorb light. Absorption of left circularly polarized (lcp) and right circularly polarized (rcp) light is associated with transitions of $\Delta J = +1$ and -1, respectively (Fig. 2.10) [10–12]. The differential absorption between lcp and rcp light, ΔA_{L-R}, is recorded as the MCD spectrum and is characterized by three terms; Faraday A, B, and C terms (Eq. 2.9), where B is the strength of the magnetic field (T), cl is the product of the concentration of the molecule (M) and optical path length (cm), and kT is the product of the Boltzmann constant and temperature (K).

$$\Delta A_{L-R} = 152.5Bcl[A + (B + (C/kT)] \tag{2.9}$$

The Faraday A term is observed when the ground state is nondegenerate whereas the excited state is degenerate in the transition. The degenerate transition is split into two transitions which are very similar in energy and during which lcp light and rcp light are absorbed. Hence, the observed CD spectrum is sharp and it appears that the first-order derivative curve of the absorption spectrum was recorded (Fig. 2.10, top).

The Faraday B term appears irrespective of whether the transition is degenerate or nondegenerate (Fig. 2.10, middle). Therefore, when neither the ground state nor the excited state is degenerate for transitions in molecules of lower symmetry (e.g., H_2Pc; see Sect. 2.2.9), the MCD spectrum is completely dominated by B terms. The B terms arise owing to the mixing between excited states that are linked by a magnetic transition moment, which is induced by the applied magnetic field. The intensity of B terms increases in inverse proportion to the energy separation between the states. The spectrum relevant to the transitions must be a "zero-sum game".

The Faraday C term (C/kT in Eq. 2.9) is observed only when the ground state is degenerate and the excited state is nondegenerate (Fig. 2.10, bottom). They are temperature-dependent because of the Boltzmann distribution between the split ground states induced by the magnetic field. Therefore, the C terms are Gaussian-shaped as is the case of B terms. However, degeneracy of ground states is not very common in phthalocyanines or related macrocycles because of the Jahn-Teller effect [13–15]. Hence, the C term is not taken up in this monograph.

MCD spectroscopy also provides information regarding the change in magnetic dipole moment through the observed transitions [16, 17]. The optical absorption and MCD spectra of some porphyrins and related macrocycles are shown in Fig. 2.11. The Q band observed for the Sb^V complex (cation) of octaethylporphyrin in the absorption spectrum is weaker than the Soret band (dotted line) commonly observed for normal porphyrins (e.g., TPP in Fig. 2.2) [18]. Nevertheless, the associated MCD spectrum has a comparable intensity. The free-electron model predicts that the Soret band is allowed and hence shows a small change in orbital angular momentum ($\Delta k = \pm 1$). In contrast, the Q-transition is forbidden but has a large Δk (± 9), which is related to the magnetic moment in the excited state.

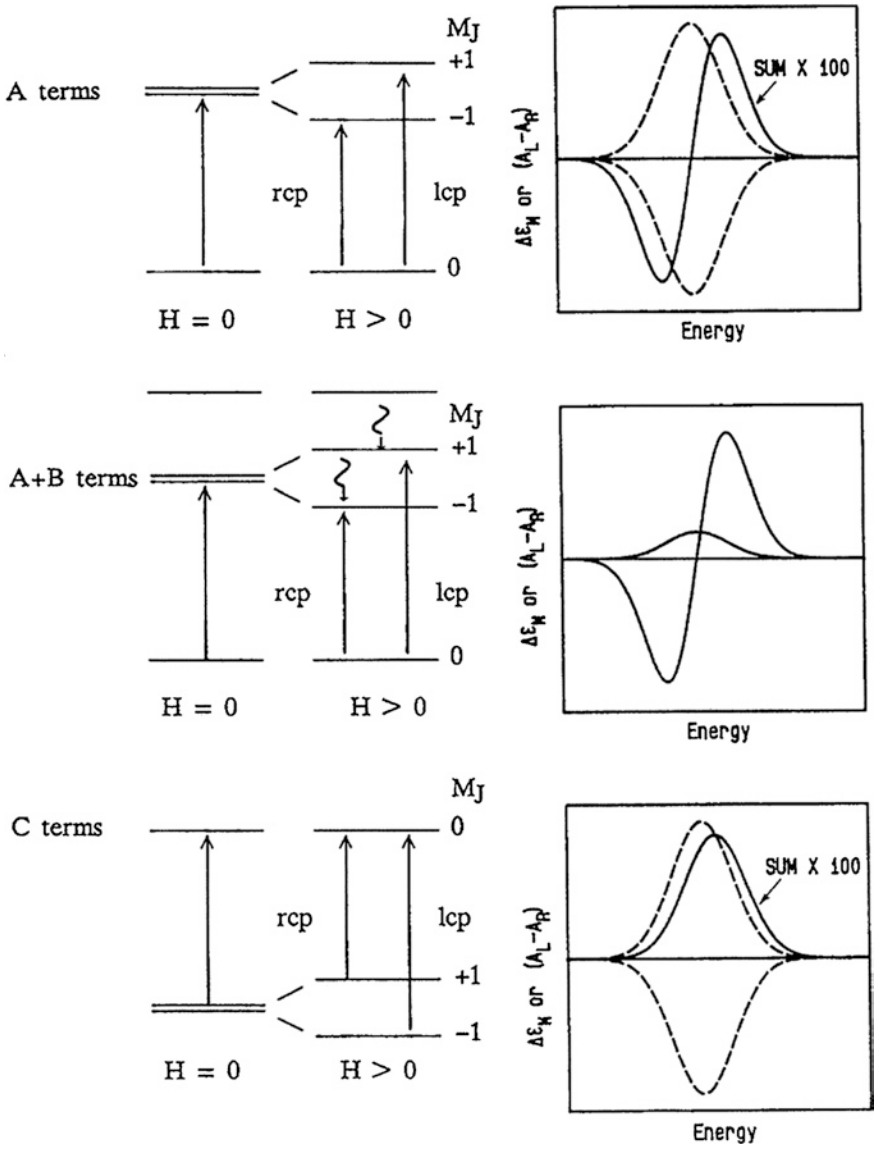

Fig. 2.10 Origin of the Faraday A, B, and C terms observed in MCD spectra. The *dashed curves* represent the absorbance of left and right circularly polarized light. "H", which stands for the magnitude of the external magnetic field, corresponds to "*B*" in the text. Reprinted from Ref. [12], Copyright 2003, with permission from Elsevier

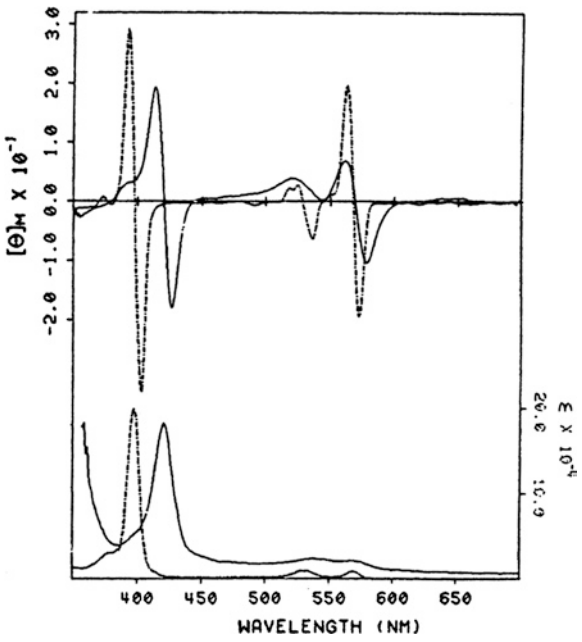

Fig. 2.11 MCD (*top*) and optical absorption spectra of purified reduced +CO P-420 at pH 7.4 (*solid lines*) and (dihydroxo) (octaethylporphyrinato) antimony(V) chloride (*broken lines*) in dichloromethane. Reprinted with the permission from Ref. [18]. Copyright 1977 American Chemical Society

2.2.9 *Assignment of Phthalocyanine Spectra by MCD Spectroscopy*

Using MCD spectroscopy, we can unambiguously assign each band observed in Fig. 2.1. The spectra of [Zn(tbpc)] and H_2tbpc will be discussed as examples of degenerate and nondegenerate transitions, respectively.

The optical absorption and MCD spectra of [Zn(tbpc)] are shown in Fig. 2.12 as black solid lines, where a distinct S-shaped curve is observed in the 650–700 nm spectral range with its center at essentially the same wavelength as that of the absorption maximum (678 nm). On this basis, we may assume that the MCD spectrum in this spectral region is dominated by a Faraday A term and hence this transition is degenerate. A similar S-shaped sigmoid curve is observed in the MCD spectrum at approximately 348 nm, indicating that this transition is also degenerate.[13] Using MCD spectroscopy, we found that the 678- and 348-nm bands are unambiguously assigned as the Q and Soret bands, respectively, as is predicted from the four-orbital model. The weak satellites at the blue flank of the Q band are

[13]For some compounds, e.g., [Zn(pc)], [Mg(pc)], [Li_2(pc)] [19–21], and some As^V and Sb^V derivatives [22–24], a similar absorption band in the spectral region has been reported but they are considered as an overlap of two bands (B1/B2 bands) on the basis of MCD spectra (Sect. 3.2.2.1).

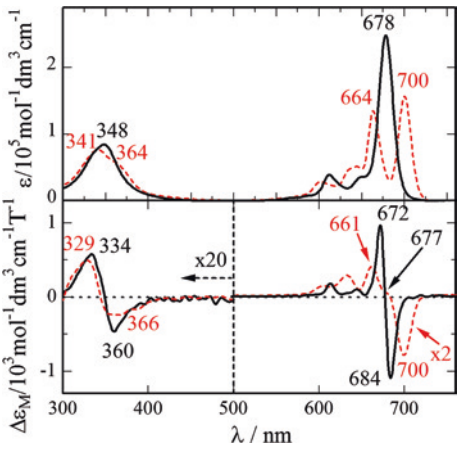

Fig. 2.12 Optical absorption (*top*) and MCD spectra of [Zn(tbpc)] (*bottom*), (*black solid lines*) and H_2tbpc (*red broken lines*) in chloroform solution. The absorption spectra are identical to those in Fig 2.1

attributed to vibronic progression (Sect. 1.1.3) associated with the Q band.[14] These bands are nondegenerate as determined from the MCD spectrum in the same spectral region, which is dominated by B terms.

Absorption and MCD spectra of H_2tbpc are shown in Fig. 2.12, where no Faraday A term is observed under each band and only Faraday B terms are observed in the MCD spectrum as a Gaussian-shaped signal that appears similar to absorption bands. This indicates that H_2tbpc does not have any degenerate excited state because of its low molecular symmetry (D_{2h}). Owing to the presence of the imino protons in the cavity (Fig. 2.2), the e_g orbitals that are degenerate in D_{4h} symmetry are split into b_{2g} and b_{3g} in D_{2h} symmetry (note that the molecular plane is again taken as the *xy*-plane.[15] Using this convention, the low and high transitions are *y*- ($A_u \times B_{2g} = B_{2u}$) and *x*-polarized ($A_u \times B_{3g} = B_{3u}$) and are hence no longer degenerate. It is not easy to determine the practical interpretations of B terms.

Careful readers may have determined that the sign of the MCD spectra in the Q-region changes from negative to positive with increasing energy (i.e., from longer to shorter wavelengths) for both A and B terms. This sequence makes sense and is observed when the energy gap between the two lowest unoccupied π-MOs (that is, adjacent LUMOs) is smaller than that between the two highest occupied π-MOs (adjacent HOMOs) [16, 17]. Readers who are interested in this issue are

[14]With respect to the second vibronic band (612 nm), Mack and Stillman have suggested the presence of an additional nondegenerate electronic (n-π) transition in this spectral region due to the lack of the corresponding band in the fluorescence spectrum [25].

[15]The convention employed for D_{2h} here is different from that of the global standard, which recommends taking the z-axis (principal axis) in the D_{2h} point group so that it passes through as many atoms as possible (i.e., the z-axis is parallel to the phthalocyanine molecular plane). This is the reason why some studies have shown that the split LUMOs belong to b_{1g} and b_{2g}. However, strictly following the standard convention might lead to unnecessary confusion in comparison with [Zn(Pc)] (D_{4h}), where the z-axis must be its C_4 axis and hence is perpendicular to the molecular plane. Therefore, the z-axis for H_2Pc has been taken similarly for easier comparison with [Zn(Pc)].

referred to Michl's original reports. This is common for porphyrins, phthalocyanines, and their related macrocyclic compounds because their LUMOs are doubly degenerate or nearly degenerate, whereas their adjacent HOMOs are separated in energy as is expected from the four-orbital model.

2.2.10 Computational Molecular Orbital Calculations

It is not our purpose in this chapter to discuss the electronic structures of phthalocyanines and related macrocycles on the basis of computational molecular orbital calculation. However, it should be mentioned that some findings are available from computational works alone. In particular, the following two findings are quite important for description of optical spectra of phthalocyanines.

First, the Q band is assigned as essentially a pure HOMO-LUMO transition (i.e., $a_{1u} \rightarrow e_g$ for [M(Pc)], and $a_u \rightarrow b_{2g}$ and $a_u \rightarrow b_{3g}$ for H_2Pc). Although the Q band transition is a mixture of $a_{1u} \rightarrow e_g$ and $a_{2u} \rightarrow e_g$ according to the four-orbital model, a large stabilizing effect of nitrogen substitution on the a_{2u} orbital as against a_{1u} significantly reduces the contribution of the a_{2u} orbital to the Q-transition [9–12, 26].

Second, three absorption bands (B, N, and L bands in the order of increasing energy) appear in the higher-energy spectral region (the so-called Soret region), and are mixtures of more than one degenerate electronic transitions [8, 10–12]. The bands of higher energy (N and L) cannot be observed in organic solvents because they are hidden owing to intense absorption by the solvents used. Their presence has been determined in the spectra of As^V and Sb^V complexes that have significantly redshifted the Q and Soret bands [22–24].

References

1. M. Sommerauer, C. Rager, M. Hanack, J. Am. Chem. Soc. **118**, 10085–10093 (1996)
2. O.S. Finikova, A.V. Cheprakov, I.P. Beletskaya, P.J. Carroll, S.A. Vinogradov, J. Org. Chem. **69**, 522–535 (2004)
3. E.S. Nyman, P.H. Hynninen, J. Photochem. Photobiol. B Biol. **73**, 1–28 (2004)
4. C. Ercolani, A.M. Paoletti, G. Pannesi, G. Rossi, A. Chiesi-Villa, C. Rizzoni, J. Chem. Soc. Dalton Trans. 1971–1977 (1990)
5. W.T. Simpson, J. Chem. Phys. **17**, 1218–1221 (1949)
6. A. Ceulemans, W. Oldenhof, C. Görller-Walrand, L.G. Vanquickenborne, J. Am. Chem. Soc. **108**, 1155–1163 (1986)
7. M. Gouterman, J. Mol. Spectrosc. **6**, 138–163 (1961)
8. M. Gouterman, G.H. Wagniere, L.C. Snyder, J. Mol. Spectrosc. **11**, 108–127 (1963)
9. C. Weiss, H. Kobayashi, M. Gouterman, J. Mol. Spectrosc. **16**, 415–450 (1965)
10. M.J. Stillman, T. Nyokong, in *Phthalocyanines: Properties and Applications*, vol. 1, ed. by C.C. Leznoff, A.B.P. Lever (VCH, New York, 1989), p. 133
11. J. Mack, M.J. Stillman, in *Porphyrin Handbook*, vol. 16, ed. by K.M. Kadish, K.M. Smith, R. Guilard (Elsevier Science, USA, 2003), pp. 43–116

12. J. Mack, M.J. Stillman, Coord. Chem. Rev. **219–221**, 993–1032 (2001)
13. J. Mack, M.J. Stillman, J. Am. Chem. Soc. **116**, 1292–1304 (1994)
14. J. Mack, S. Kirkby, E. Ough, M.J. Stillman, Inorg. Chem. **31**, 1717–1719 (1991)
15. J. Mack, M.J. Stillman, Inorg. Chem. **36**, 413–425 (1997)
16. J. Michl, J. Am. Chem. Soc. **100**, 6801–6811 (1978)
17. J. Michl, Tetrahedron **40**, 3845–3934 (1984)
18. J.H. Dawson, J.R. Trudell, G. Barth, R.E. Linder, E. Bunnenberg, C. Djerassi, M. Gouterman, C.R. Connell, P. Sayer, J. Am. Chem. Soc. **99**, 641–642 (1977)
19. E. Ough, T. Nyokong, K.A.M. Creber, M.J. Stillman, Inorg. Chem. **27**, 2724–2732 (1988)
20. M.J. Stillman, A.J. Thomson, J. Chem. Soc. Faraday Trans. **II**(70), 805–814 (1974)
21. T.C. VanCott, J.L. Rose, G.C. Misener, B.E. Williamson, A.E. Schrimph, M.E. Boyle, P.N. Schatz, J. Phys. Chem. **93**, 2999–3011 (1989)
22. H. Isago, Y. Kagaya, Inorg. Chem. **51**, 8447–8454 (2012)
23. H. Isago, Y. Kagaya, J. Porphyrins Phthalocyanines **13**, 382–389 (2009)
24. H. Isago, Y. Kagaya, H. Fujita, T. Sugimori, Dyes Pigm **88**, 187–194 (2010)
25. J. Mack, M.J. Stillman, J. Phys. Chem. **99**, 7935–7945 (1995)
26. N. Kobayashi, H. Konami, in *Phthalocyanines: Properties and Applications*, vol. 4, ed. by C.C. Leznoff, A.B.P. Lever (VCH, New York, 1996), p. 343

http://www.springer.com/978-4-431-55101-0

Optical Spectra of Phthalocyanines and Related Compounds

A Guide for Beginners

Isago, H.

2015, X, 132 p. 79 illus., 41 illus. in color., Softcover
ISBN: 978-4-431-55101-0